Investigation about the effect of angle of attack and relative humidity on wheel squeal

Liu X., Bellette P., Milne C. and Meehan P.A.

School of Mechanical and Mining Engineering, The University of Queensland, Brisbane, Australia

ABSTRACT

In order to validate prediction models of wheel squeal, a two-disk rolling contact test rig has been developed to investigate fundamental squeal behaviour. This test rig has been modified to allow for a range of angles of attack to be set and measured accurately, with a relative error about 1%. On the other hand, in order to perform a controlled investigation of the effects of humidity on wheel squeal, a humidity control system was set up in the enclosure of the test rig. Squeal noise was recorded at the different angle of attack, rolling speed and relative humidity, and the analysed results not only indicate the effect of these parameters initially, but also correlate well with the results from modal test and FEA. Furthermore, the test rig was retrofitted to measure the lateral force at the rolling contact patch with strain gauges on leaf springs.

INTRODUCTION

Squeal noise is a kind of high level tonal noise generated by a train passing a curve of the rail, to which human's ear is very sensitive due to its unique characteristics. With rising living standards, people are less likely to tolerate noise, and consequently, the investigation into railway noise has been carried out globally around the world. Legislation for noise emission from trains and track is quite new and currently limited to a few countries; and legislation of this type will come into force in more countries in the future. Austria set noise emission limits for single vehicles in 1993, and reduced the emission limits of freight wagons by 10 dB in 2002. Italy's emission limits came into force in 2002 and will reduce 2 dB further by 2012. Some countries, like Germany and Switzerland, are legislating for railway noise emission. Legal limits on the noise emitted by individual rail vehicles have been introduced in Europe since 2002. Furthermore, the Environmental Noise Directive required the production of noise maps of existing sources and to develop action plans to reduce noise in identified spots. As to Australia, the RailCorp is required to keep the maximum level under 60 dBA LAeq (24hour), and work towards a planed level of 55 dBA.

In the last two decades, curve squeal has been investigated theoretically and experimentally, so different kinds of countermeasures have been proposed, including damping treatment to wheel or rail, bogie skirt, friction modifier, etc. Among these methods, friction modifier is reasonably effective especially for high frequency noise (Kalousek, 2005). However, one problem is that the SPL (sound pressure level) of the squeal noise cannot be measured until the line is in operation, when it is already quite late and costly to make these kinds of modification. On the other hand, due to legislation regarding noise emission, manufacturers need to consider the noise reduction in advance in the design process. Therefore, it is strongly desirable to predict the sound pressure level of squeal noise, in order to provide guidance in combating railway noise.

Up to now, some models of curve squeal have been proposed, most of which are based on the squeal mechanism summarized by Rudd(Rudd, 1976): it is the stick-slip phenomenon due to the variation of rolling contact friction coefficient with lateral creepage in the wheel/rail contact that leads to the tonal squeal noise. The mechanical model of a friction oscillator excited by a moving base is illustrated in Figure 1.

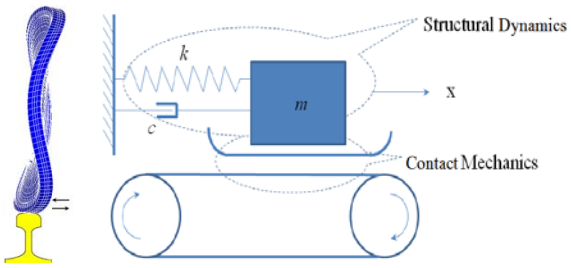

Figure 1. Single degree of freedom friction driven mechanical oscillator

It is a SDOF model of a massive block placed on a rigid belt moving with constant velocity and a spring with a stiffness of *k* restraining the mass. As the spring is extended, the friction force between the mass and belt increases with the displacement, until the static friction force reaches its maximum in amplitude, and the mass begins to slide. Then the friction force drops to the value of kinetic friction force between the mass and the belt, and the spring force starts to decrease with the moving of block. When the block sticks to the belt again, the spring force and the kinetic friction force reach a new balance. In the case of curve squeal, the top surface of the rail move in the lateral direction with respect to the wheel and it can be taken as the moving belt in Figure 1. The wheel, with its own stiffness and damping, forms a structural dynamic system on the top of the rail. Due to the difference between the static friction coefficient and kinetic friction coefficient at the contact point, this kind of stick-slip phenomenon will also happen at certain frequencies. Particularly, the wheels can vibrate in a high frequency comparatively, since the wheels generally have higher dynamic stiffness.

This kind of rolling contact theory was introduced by Hertz and extended by Johnson and Vermeulen(Johnson, 1985) in the three-dimensional case. The contact surface between two rolling bodies can be divided into two regions, the slip region and the stick region. Kalker has summarized the theories of Johnson, Shen and Hedrick, etc., and included spin creepage to calculate the creep force(Kalker, 1991, Kalker, 1990). This

theory was applied by Hsu to investigate the relationship between the squeal phenomenon and the properties of the adhesion coefficient (Hsu et al., 2007). A model for lateral force at the wheel/rail contact proposed by Beer (de Beer et al., 2003) is more comprehensive, integrating more relevant parameters involved. To date, however, the high levels of creepage beyond the saturation regime of contact forces have not been included to form part of dynamic simulation packages, but it is the region where negative damping exists in the creep curve. Kinds of assumptions about the creep curve, however, have been proposed, which are quite different especially in falling region. For the convenience of comparison, the friction characteristics used in models of curve squeal are plotted in Figure 2.

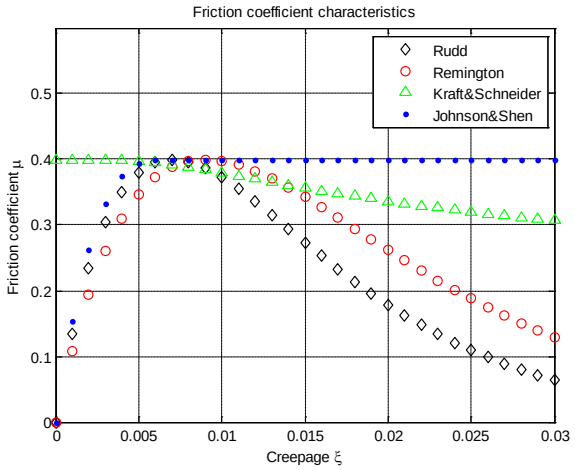

Figure 2. Friction characteristics used in different models

The formula expressions of Rudd and Remington are similar, only that Rudd took critical creepage as 0.7%, while for Reminton's theory is 0.9%. The model of Kraft and Schneider describes merely the creep curve in the falling part. As to the model presented by Jonson and Shen, it has integrated Kalker's theory about rolling contact and the effect of contact patch dimensions, which makes it more advanced in simulating the real situation.

TWO DISKS ROLLING CONTACT TEST RIG

To investigate the phenomenon of squeal noise, a two disk rolling contact test rig is applied, whose picture is displayed in Figure 3.

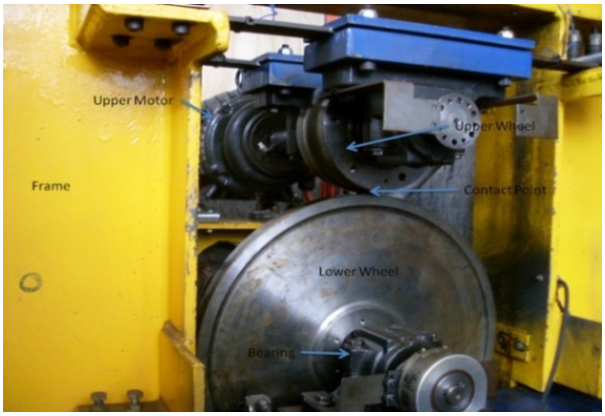

Figure 3. Front view of the two disk rolling contact test rig

Its upper wheel and lower wheel are driven by a vector controlled constant speed motor and constant torque motor, respectively. The yaw angle of the lower wheel with respect to the frame can be adjusted to simulate the yaw angle of the misalignment between the directions of rolling speed and the tangential direction of the rail. The vertical force can be adjusted by spacers at both ends of leaf springs. Strain gauges were installed on leaf springs to measure the vertical loading, and a temperature sensor was installed on the frame near the lower wheel. A summary of parameters of this test rig can be found in Table 1.

Table 1. Test Rig Parameters

Description	Value
Lower Disk Radii of curvature (longitudinal, lateral)	0.213 m, 0.300 m
Thickness of the lower wheel	0.015m
Mass per unit area of lower wheel	117.75kg/m^2
Inside radius of lower wheel	0.0325m
Modulus of elasticity of lower wheel	200GPa
Upper Disk Radii of curvature (longitudinal, lateral)	0.085 m, 0.040 m
Normal Force Range (P_0)	0 - 2000 N
Tangential Load Range (Q_0)	0 - 1000 N
Contact Velocity Range	0 - 26.8 m/s
Lower Disk Rolling Speed	0 – 1200 RPM
Disk Material	Cast Steel (0.71% C, 0.46% Si, 0.85% Mn, 0.05% Cr, 0.02% Ni, 0.01% Mo. 0.02% S, 0.02% P)
Yield Strength	420 MPa
Density (ρ)	7800 kg/m^3
Poisson's Ratio (ν)	0.28

In order to acquire dynamic characteristics of the wheel, impact hammer tests have been conducted to the lower wheel. An impact hammer test is a type of modal test where a hammer is used to excite an object in order to determine its natural frequencies, modal damping and modal shapes. After analysing the results, the receptance of the wheel can be calculated. Receptance is like a spectrum of dynamic stiffness and a measurement of movement for a given force at each frequency. For these tests, the upper disk was jacked up or dismounted so as not to contact the lower disk, so vibrations of the lower disk were isolated from ambient objects. All tests were carried out using a hard tip hammer to strike the edge of lower wheel laterally and two accelerometers attached to different positions on the wheel with small magnets. Positions for accelerometer attachment and hammer striking on the lower wheel are marked in Figure 4.

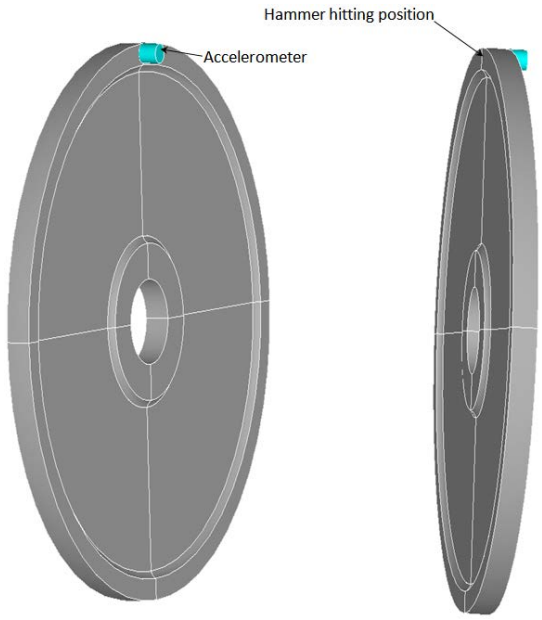

Figure 4. Positions of accelerometers and struck place

One spectrum acquired from data attained from an impact hammer test is displayed in Figure 5, which can show the lateral receptance of the wheel at different frequencies. Those peaks in the spectrum are indicating the dominant frequencies of the wheel when vibrating laterally.

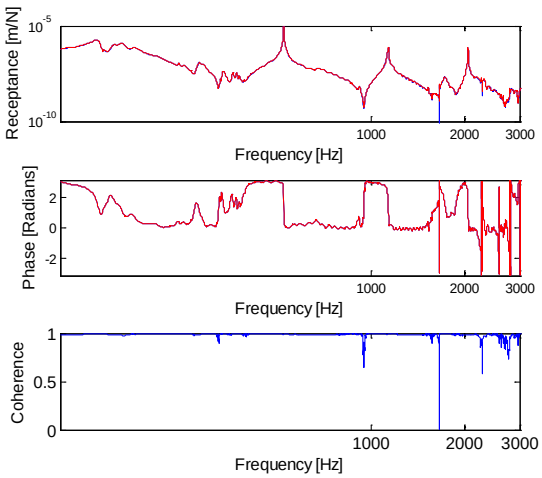

Figure 5. Lateral receptance of the wheel

On the other hand, a theoretical prediction about the vibration of the wheel for the test rig was conducted, based on the equation for an annulus (Blevins, 1979), which makes it possible to calculate fundamental frequencies and relevant mode shapes. The boundary conditions are those of being clamped around the inner circumference and free around the outer circumference. It includes no effects of shear deformation, rotary inertia or gyroscopic effects under rolling. The formula used in this analysis is applicable to linear elastic homogeneous, isotropic material and the deformations are small in comparison with the thickness. With the assumption above, the natural frequencies of a plate in different mode shapes can be calculated with,

$$f_{ij} = \frac{\lambda_{ij}^2}{2\pi a^2}\left[\frac{Eh^2}{12\gamma(1-\upsilon^2)}\right]^{\frac{1}{2}}, \quad i = 0,1,2,\cdots;\ j = 0,1,2,\cdots; \qquad (1)$$

Where f = natural frequency (Hz); λ = dimensionless frequency parameter; a = outside radius; b = inside radius; h = plate thickness; i = number of nodal diameters; j = number of nodal circles; E = modulus of elasticity; γ = mass per unit area of plate; v = Poisson's ratio.

The resonant frequencies for lateral modal shapes of the lower wheel can be calculated by equation 1, with reference to the parameters listed in Table 1. For five fundamental modal shapes, their corresponding frequencies are calculated and listed in Table 2.

Table 2. Calculated resonant frequencies

i	j	λ^2	Frequency (Hz)	Mode Shapes
0	0	4.87	393.5	
1	0	4	323	
2	0	6.2	500	
3	0	12.6	1017	
0	1	29.88	2412	

In this table, the resonant frequency for mode (3, 0) can be calculated as 1017 Hz. This is likely to be the dominant frequency in the sound radiation, since this kind of modal shapes, having zero nodal circle and more than two diameters, are very efficient in the sound radiation. In comparison with spectrum of lateral vibration in Figure 5, it is quite close to the dominant frequency around 1100 Hz, only that this calculated frequency is a bit lower than that of the modal test. It is because the thickness of the wheel used in the calculation is the value of web, which has the largest area but the thinnest thickness of the wheel, so it makes the calculated frequency also a bit low. Furthermore, a squeal model focusing on the vibration was developed using a single degree of freedom description of the dominant lateral vibration mode (P.A.Meehan et al., 2011). The analysis proved that the squeal noise of the testrig is mainly associated with transverse modes of lower wheel's vibration.

EXPERIMENTAL METHODOLOGY FOR INVESTIGATION OF SQUEAL NOISE PARAMETERS

Up to now, the sound pressure level of squeal noise cannot be predicted accurately yet, partly because it is subject to several factors, including AoA (angle of attack), normal loading, running speed and humidity, etc. In this research, series of experiments about this have been conducted on the test rig, whose results are summarized here.

Angle of attack

If the creep coefficient is constant, the lateral creep force is determined only by the yaw angle. It is believed that the non-zero yaw gives rise to a lateral velocity component that is converted into a contact force by the force-creepage relationship. This force cannot grow forever and will saturate the adhesion at the contact patch between the wheel and rail, leading to possible stick-slip phenomena, whose generation mechanism has been illustrated in Figure 1. Therefore, it

looks like the yaw angle between the wheel and rail is a pre-requisite for the generation of squeal noise. To investigate the effect of angle of attack to squeal noise, the test rig has been modified by cutting slots at connections of motor and brackets as shown in Figure 6. This allows the lower wheel and the motor connected to it to rotate about the vertical axis of the two wheels between -6 mrad and 32 mrad.

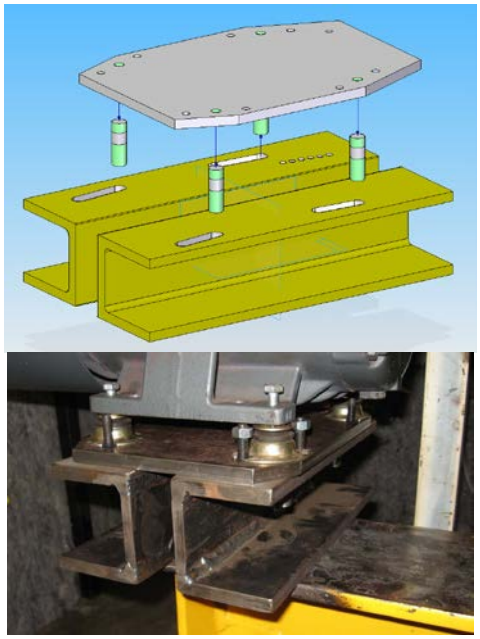

Figure 6. Adjustable motor mount for variable AoA

Initially, the angle of attack was measured with a conventional method by measure five dimensions as illustrated in Figure 7. Then the angle can be calculated with the geometric relationship of these measured values.

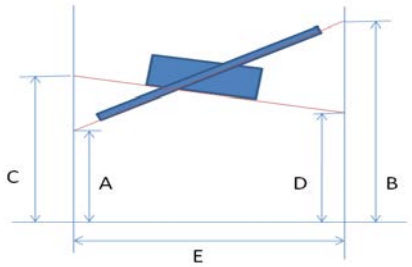

Figure 7. Measurement of AOA with conventional method

Since this method needs to measure five dimensions, the relative error of calculated angle is reasonably appreciable due to so many measurements, which is up to 6%. Therefore, a laser distance measurer (Bosch DLE70) is applied to measure the angle of attack as illustrated in Figure 8.

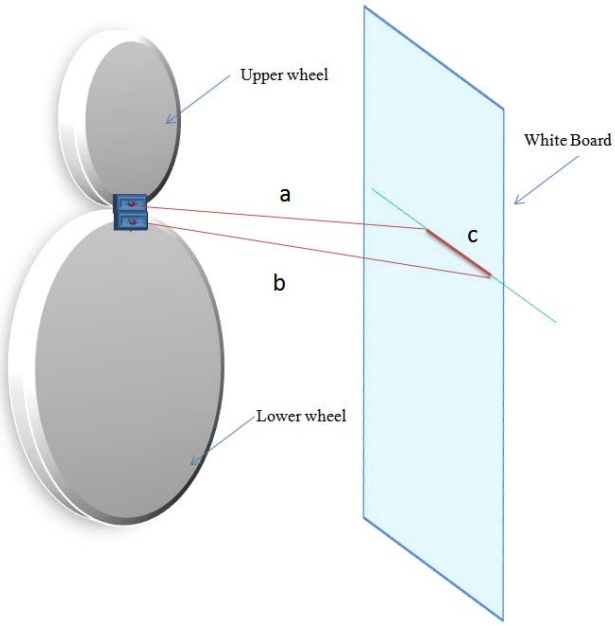

Figure 8. New method of measuring angle of attack

This device can project a laser beam to a vertical plane at a distance of about 6 meters away from the facade of test rig's wheels. Two points can be projected to the plane from the upper and lower wheel, respectively. Simultaneously, the laser distance measurer can record the distance from the wheel to the white board, then the angle of attack can be calculated after measuring the distance between the two points on the white board. With this method, the relative error of AOA measurement can be reduced to 1%, which has increased the accuracy prominently.

Humidity

It is found that the presence of humidity and vibration can affect the friction coefficient (Chowdhury and Helali, 2006). Generally, the friction coefficient would drop down with the increase of humidity, because the water can reduce the coefficient when two disks rolling against each other for a range of relative humidity. When taking RH% as the percentage relative humidity, a linear approximation of this experimental data was yielded (P.A.Meehan et al., 2010):

$$\mu = \mu_D \times (1 - 0.0022RH\%) \quad (2)$$

Where, μ_D is the general friction coefficient without the consideration of the effect of humidity.

To investigate the effect of humidity on wheel squeal, a humidity control and measurement system was set up in the acoustic enclosure of the test rig. It mainly consists of an atomiser (Condair 505) used as a humidifier to increase the humidity by releasing a fine aerosol mist of evaporated water particles, a dehumidifier (MoistureCure 735 EA-30R) with a built-in humidistat to control humidity, and a logger (Testo 175-H2) to record the humidity level and temperature (cf. Figure 9). With this system, the relative humidity can be adjusted between 45% and 95%.

Figure 9. Condair 505 Atomiser (left), MoistureCure 735 EA-30R dehumidifier (middle) and Testo 175-H2 humidity/temperature logger (right)

On the other hand, field measured trends for the effect of relative humidity on the coefficient of friction have been able to be predicted using a relatively simplified wheel squeal model that suitable for probabilistic measurements (P.A.Meehan et al., 2010). This probabilistic theoretical model is reasonably effective in matching the trend of the effect of relative humidity on the probability of wheel squeal.

Lateral force measurement

At present, a method to measure the lateral force is developed with strain gauges on surfaces of leaf springs. The vertical loading on the leaf springs can be measured with 16 strain gauges installed on the upper and lower surface of the leaf spring. All strain gauges are applied basing on the Wheatstone full-bridge configuration. It is a network of four resistive legs. The output of this bridge can be measured between the middle nodes of the two voltage dividers. This configuration can give maximum bending strain output ignoring axial strain and twisting of the leaf spring. It can also provide maximum thermal compensation during measurement to eliminate the effect temperature has on the change in resistance of sensing elements.

A lateral force applied on the edge of the upper wheel will increase the vertical force of the outer leaf spring and decrease that of inner leaf spring. The reliability of this method has been investigated with FEM. DOF at both ends of leaf springs haven been constrained, while at the end of the axle only one freedom of rotation is available. The geometric and material characteristics of the leaf springs, axle and rubber coupling have been given sufficient consideration. When lateral force is applied on the wheel, it will result in a difference in the deformation of leaf springs in the vertical direction as illustrated in Figure 10.

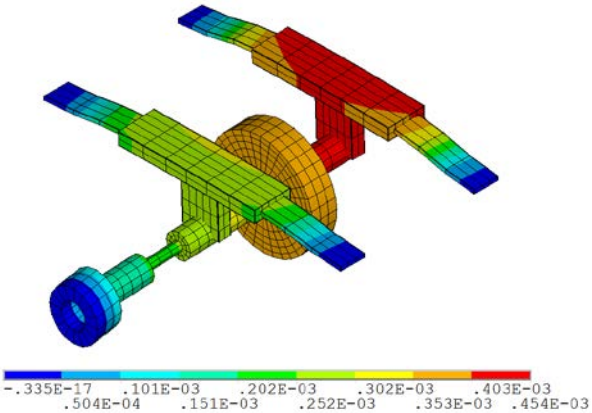

Figure 10. Vertical deflection of the structure (m)

Results from finite element analyses can assure the feasibility of measuring the lateral force in rolling contact with strain gauges on leaf springs. The leaf spring is also modelled with Ansys, and the strain of the leaf spring in the longitudinal direction is plotted in Figure 11.

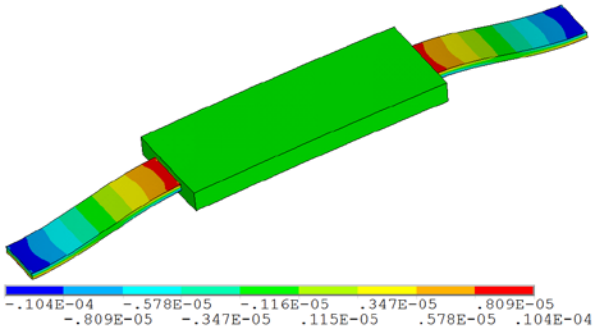

Figure 11. The strain of one leaf spring in the longitudinal direction

Strain gauges are attached on the top surface and bottom surface the leaf spring in this figure, so the change of strain under different lateral forces can be recorded. The deflections of leaf springs are reasonably small, the relationship between the lateral force and the difference of strain on those two leaf springs can be determined with calibration.

RESULTS

With a normal loading of about 600 N, the sound generated by the test rig was recorded with a microphone (Bruel & Kjaer 4134), placed approximately 15cm away from the facade of the lower wheel in a perpendicular position. The yaw angle between the upper wheel and lower wheel was adjusted by moving the motor of the lower wheel about the vertical axis of two wheels. When the upper wheel and the lower wheel were set at a series of yaw angles from zero mrad to 30 mrad, the sound was recorded and analysed as illustrated in Figure 12.

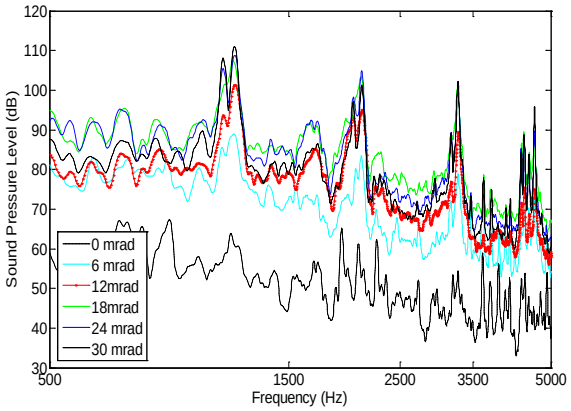

Figure 12. Effect of AoA on squeal noise

It is evident that the sound pressure level increases with the angle of attack initially. This trend, however, is not that obvious when the yaw angle reaches a certain value, in another word, the SPL of 18 mrad, 24 mrad and 30 mrad are almost similar. Another interesting phenomenon is that when the yaw angle exceeds six mrad, the spectrum already shows the trend of discrete distribution in the frequency domain, so the critical creepage in this experiment should be around six mrad.

To investigate the effect of rolling speed to squeal noise, experiments were conducted on the test rig and the generated sound was recorded when the test rig was running. With the normal force of 300N and angle of attack about 24 mrad, the sound produced by the squeal noise was recorded from 100 RPM to 700 RPM. As illustrated in Figure 13, the result shows that sound pressure level will increase from about 90 dB to 120 dB correspondingly.

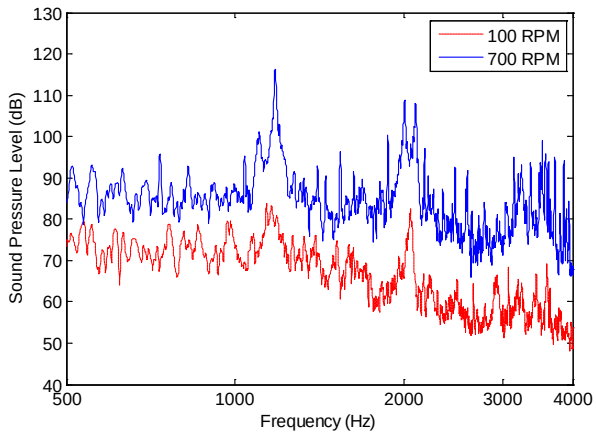

Figure 13. Effect of speed on curve squeal

Obviously, in the spectrum of 700 RPM, it can be seen that the peaks in the sound spectra correspond well to the peaks in the receptance peaks from modal tests as shown in Figure 5. This provides strong evidence that the squeal noise is associated with the transverse vibration modes of the larger lower disk.

As to the test about humidity, even though the effect is not as evident as AoA or rolling speed, the difference still can be detected. For example, at the yaw angle of 12 mrad, when the relative humidity was increased from 45% to 95 %, the one-third octave spectra at the dominant frequency band of 1250 Hz at different speeds was compared as illustrated in Figure 14. It shows that the SPL does not appear to be affected by changes in relative humidity until the relative humidity reached 95%, where there is a significant drop in SPL. This might because when the relative humidity reaches certain level, enough water is accumulated on the wheel contact surface to create a thin film of moisture and contaminant, which can affect the friction dramatically.

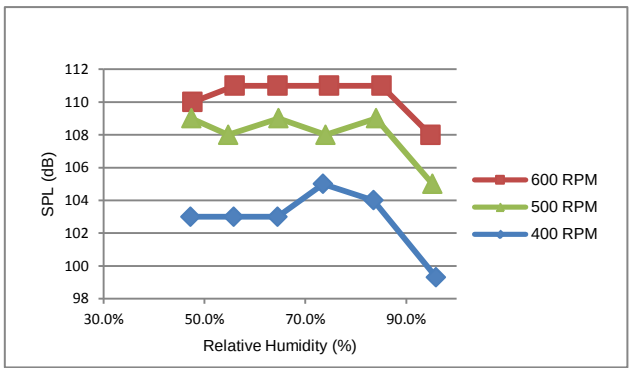

Figure 14. Effect of humidity on squeal (Osborne, 2010)

With strain gauges installed on leaf springs, the lateral force and normal loading can be measured in different rolling speed, from 100 RPM to 600 RPM with an increment of 100 RPM. Since the normal loading and the lateral force are measured simultaneously with the same batch of data, the traction ratio can be calculated reliably. The average value of the traction ratio at different speeds is illustrated in Figure 15. It is plotted with nonlinear least squares fit to a creep-force model and a confidence interval of 95% as marked by dashed lines in the figure. When the test rig ran at 600 RPM (13.36 m/s), obvious squeal phenomenon can be observed when the angle of attack is larger than 6.8 mrad, where the sound pressure level at a dominant frequency around 1200 Hz can be higher than 100 dB.

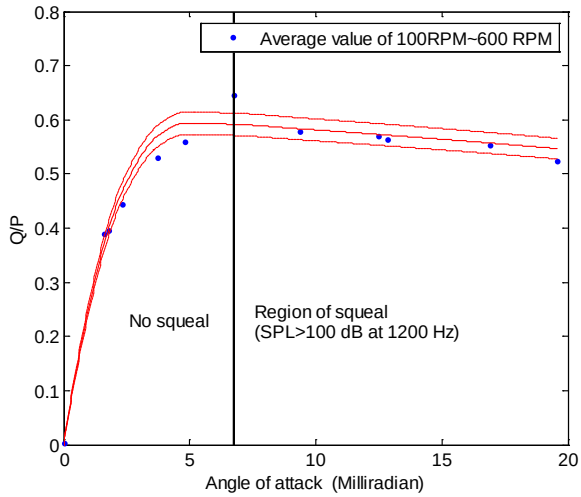

Figure 15. Averaged traction ratio (100 RPM~600RPM) in rolling contact at different AoA and the effect of lateral forces on squeal occurrence, -- is confidence interval of 95%

An analysis to the error of this measurement indicates that this method has an error tolerance of about 3.6% and 3.8% for lateral and vertical force measurement, respectively. Then the error tolerance of the traction ratio can be calculated as 5.3%. This error analysis shows that this method can measure vertical and lateral force with reasonable accuracy.

CONCLUSION

The dynamic characteristic of the wheel has been investigated experimentally, which corresponds well with the analysis of sound spectra in the frequency domain. In comparison with spectra of recorded sound in the test, it is reasonably evident that the dominant frequency can be spotted around frequencies similar to spectra acquired with modal test. Therefore, when lateral force acts in frequencies near these frequencies, it tends to excite vibrations contributing significantly to the SPL of squeal noise.

Currently, the modification to the test rig makes it possible to introduce a yaw angle between two rolling wheels in the test rig, so as to simulate a wheel of a train passing the curve of track. The generated noise can be measured accurately with a laser distance measurer with a relative error of 1 %. Atomiser and dehumidifier are applied to control relative humidity inside the acoustic enclosure of the test rig, with which the relative humidity can be adjusted between 45% and 95%. Initial results can reveal qualitatively the effect of humidity to SPL of squeal noise. Comparing the results of modal test and spectra of squeal noise, one can see that dominant frequencies recognized in the analysis of these two tests correlate well with each other. This indicates that these methods are reliable for the investigation of squeal noise.

The newly designed method cannot only measure the lateral force, but also the vertical force simultaneously, so it is quite effective in determining the traction ratio in rolling contact. The feasibility of this method, using strain gauges to measure the lateral force has also been verified with the finite element method. The analysis of the data acquired with this method shows that the traction ratio will drop down with the increase of lateral creepage. Obvious squeal phenomena can be observed in the analysis of sound spectra when the angle of attack is beyond 6.8 mrad. Further test will be conducted to investigate the starting point of squeal noise.

ACKNOWLEDGEMENTS

The authors are grateful to the CRC for Rail Innovation for the funding of this research. The authors are very grateful for the support of the Rail CRC, RailCorp, Australian Rail Track Corporation PN and QR and all other members of the project steering committee, including University Of Woolongong researchers, led by Dave Anderson. Particularly, the first author is very grateful to the financial support from CSC (China Scholarship Council).

REFERENCES

Blevins, R. D. 1979. *Formulas for natural frequency and mode shape,* New York, Van Nostrand Reinhold Co.

Chowdhury, M. A. & Helali, M. M. 2006. The effect of frequency of vibration and humidity on the coefficient of friction. *Tribology International,* 39**,** 958-962.

De beer, F. G., Janssens, M. H. A. & Kooijman, P. P. 2003. Squeal noise of rail-bound vehicles influenced by lateral contact position. *Journal of Sound and Vibration,* 267**,** 497-507.

HSU, S. S., Huang, Z., Iwnicki, S. D., Thompson, D. J., Jones, C. J. C., Xie, G. & Allen, P. D. 2007. Experimental and theoretical investigation of railway wheel squeal. *Proceedings of the Institution of Mechanical Engineers Part F-Journal of Rail and Rapid Transit,* 221**,** 59-73.

Johnson, K. L. 1985. *Contact Mechanics,* London, cambridge university press.

Kalker, J. J. (ed.) 1990. *Three-Dimensional Elastic Bodies in Rolling Contact,* Dordrecht, Boston, London: Kluwer Academic Publishers.

Kalker, J. J. 1991. Wheel-rail rolling contact theory. *Wear,* 144**,** 243-261.

Kalousek, J. 2005. Wheel/rail damage and its relationship to track curvature. *Wear,* 258**,** 1330-1335.

Osborne, T. 2010. *Investigating the effects of Humidity on Wheel Squeal in Trains.* Bechelor, The Univeristy of Queensland

P.A.Meehan, P.A.Bellette, C.Jones & D.Anderson 2010. Probabilistic prediction of wheel squeal under field humidity variation. *Proceedings of 20th International Congress on Acoustics, ICA 2010.* Sydney, Australia.

P.A.Meehan, P.A.Bellette, X.Liu, C.Milne & D.Anderson 2011. Investigation of Wheel Squeal Characteristics using a Rolling Contact Two Disk Test Rig. *9th World Congress on Railway Research.* Lille.

Rudd, M. J. 1976. Wheel/rail noise--Part II: Wheel squeal. *Journal of Sound and Vibration,* 46**,** 381-394.